QRB Discovery

www.cambridge.org/qrd

Energy landscapes and heat capacity signatures for peptides correlate with phase separation propensity

Nicy[1], Rosana Collepardo-Guevara[1,2,3], Jerelle A. Joseph[4] and David J. Wales[1]

[1]Yusuf Hamied Department of Chemistry, University of Cambridge, Cambridge, UK; [2]Department of Physics, University of Cambridge, Cambridge, UK; [3]Department of Genetics, University of Cambridge, Cambridge, UK and [4]Department of Chemical and Biological Engineering, Princeton University, Princeton, NJ, USA

Research Article

Cite this article: Nicy, Collepardo-Guevara R, Joseph JA, Wales DJ (2023). Energy landscapes and heat capacity signatures for peptides correlate with phase separation propensity. *QRB Discovery*, **4**: e7, 1–11
https://doi.org/10.1017/qrd.2023.5

Received: 27 April 2023
Revised: 09 July 2023
Accepted: 17 July 2023

Keywords:
energy landscapes; liquid-liquid phase separation; global optimisation; discrete path sampling

Corresponding authors:
Jerelle A. Joseph and David J. Wales;
Emails: jerellejoseph@princeton.edu; dw34@cam.ac.uk

Abstract

Phase separation plays an important role in the formation of membraneless compartments within the cell and intrinsically disordered proteins with low-complexity sequences can drive this compartmentalisation. Various intermolecular forces, such as aromatic–aromatic and cation–aromatic interactions, promote phase separation. However, little is known about how the ability of proteins to phase separate under physiological conditions is encoded in their energy landscapes and this is the focus of the present investigation. Our results provide a first glimpse into how the energy landscapes of minimal peptides that contain π–π and cation–π interactions differ from the peptides that lack amino acids with such interactions. The peaks in the heat capacity (C_V) as a function of temperature report on alternative low-lying conformations that differ significantly in terms of their enthalpic and entropic contributions. The C_V analysis and subsequent quantification of frustration of the energy landscape suggest that the interactions that promote phase separation lead to features (peaks or inflection points) at low temperatures in C_V. More features may occur for peptides containing residues with better phase separation propensity and the energy landscape is more frustrated for such peptides. Overall, this work links the features in the underlying single-molecule potential energy landscapes to their collective phase separation behaviour and identifies quantities (C_V and frustration metric) that can be utilised in soft material design.

Introduction

Biomolecular condensates are membraneless organelles within the cell that are thought to form via phase separation of proteins and nucleic acids (Brangwynne *et al.*, 2009; Banani *et al.*, 2017; Boeynaems *et al.*, 2019; Mittag and Pappu, 2022). Intrinsically disordered proteins are found ubiquitously in naturally occurring phase-separating proteins and the flexible nature of these proteins promotes transient interactions required for phase separation (Jonas and Izaurralde, 2013; Malinovska *et al.*, 2013; Quiroz and Chilkoti, 2015; Schmidt and Görlich, 2015; Uversky *et al.*, 2015; Pak *et al.*, 2016; Harmon *et al.*, 2017; Dignon *et al.*, 2018; Schuster *et al.*, 2020). Mutational studies have shown that π–π (aromatic–aromatic) and cation–π (cation–aromatic) interactions promote biomolecular phase separation, especially those involving tyrosine (Y), phenylalanine (F), and arginine (R) (Nott *et al.*, 2015; Brady *et al.*, 2017; Lin *et al.*, 2017; Qamar *et al.*, 2018; Wang *et al.*, 2018; Fisher and Elbaum-Garfinkle, 2020; Greig *et al.*, 2020; Martin *et al.*, 2020; Bremer *et al.*, 2022). In addition, it has been demonstrated that some residues act as 'stickers' and promote phase separation, while other residues known as 'spacers' favour the solubility of proteins (Harmon *et al.*, 2017, 2018; Holehouse and Pappu, 2018a). While at first glance, some stickers may contain similar functional groups, they can be unequal contributors to biomolecular phase separation. For instance, Y is better than F and R is better than lysine (K) in stabilising condensates (Nott *et al.*, 2015; Brady *et al.*, 2017; Lin *et al.*, 2017; Qamar *et al.*, 2018; Wang *et al.*, 2018; Fisher and Elbaum-Garfinkle, 2020; Greig *et al.*, 2020; Martin *et al.*, 2020; Bremer *et al.*, 2022). R may also modulate phase separation in a context-dependent manner (Bremer *et al.*, 2022). Some of these observations raise an important question: what are the key features that characterise the underlying energy landscapes of phase-separating proteins? In this paper, we address this question by applying the energy landscape framework to peptides with different sequences encoding π–π and cation–π interactions that are known to promote phase separation of proteins yielding biomolecular condensates. The energy landscape framework allows us to explore the potential energy landscape of the peptides by performing geometry optimisation to identify local minima and transition states, and connecting them via steepest-descent pathways (Wales, 2003). This approach provides a powerful

tool to explain emergent observable properties in terms of the atomic interactions at a fundamental level.

Specifically, we performed a computational analysis of the potential energy landscape for various hexapeptide monomers modelled at the atomistic scale. We chose hexapeptides because the secondary structure of pentapeptides is context-dependent, that is, the same sequence of five amino acids can occur in different secondary structures, such as α-helix and β-sheet (Kabsch and Sander, 1984). Therefore, hexapeptides may represent the minimal system useful for investigating the conformational properties of peptides, as well as the intramolecular interactions between the amino acids within a peptide monomer. In the stickers-and-spacers model, the 'stickers' are the interaction sites that can either be single amino acids, groups of residues, or entire domains that promote phase separation, and 'spacers' favour the solubility of proteins (Harmon *et al.*, 2017; Holehouse and Pappu, 2018b; Yang *et al.*, 2019). Following the stickers-and-spacers model, the hexapeptides are chosen to contain two dipeptide stickers joined together by a glycine–glycine (GG) spacer (Abbas *et al.*, 2021). Working with such minimal systems allows us to directly link the differences in the energy landscapes to specific interactions between amino acid pairs, and hence, reduce the impact of cooperative and competitive effects.

A key signature of the energy landscape of a molecule is its heat capacity (C_V). Previous simulations of clusters have shown that low-temperature peaks in C_V represent solid–solid transitions between alternative low-energy conformations that differ significantly in terms of their enthalpy and entropy (Doye and Wales, 1995, 1998; Doye *et al.*, 1998; Doye and Calvo, 2002; Bogdan *et al.*, 2006). In this contribution, we exploit the capability to produce rapid analysis of the heat capacity and assign the peaks to specific local minima with distinct intramolecular interactions. Measurement of C_V, as a function of temperature, can be useful to gain better insight into the thermodynamic properties of biopolymers, using differential scanning calorimetry (Benzinger, 1971; Poland, 2001, 2002; Prabhu and Sharp, 2005; Cooper, 2010). In general, low temperature C_V measurement is useful for entropy calculation (Giauque and Johnston, 1929) and for accessing vibrational modes of the molecule that are otherwise inaccessible to spectroscopic techniques that provide information about optical vibrational modes. These modes provide information about molecular conformations and stabilising interactions (Mrevlishvili, 1979). Even though biological molecules are not functional at extreme temperatures, thermodynamic analysis can offer new insights into the properties and behaviour that may have relevance at physiological temperatures. This analysis is similar to the study of crystalline (Starkweather, 1960) and amorphous polymers at low temperatures (Warfield and Petree, 1962). Specific heat measurements for peptides at low temperatures (1.8–20 K) can be employed as a measure of the elasticity of the molecule (Finegold and Cude, 1972). Here, we calculate the C_V of peptide monomers using the harmonic superposition approximation (Wales, 2017), and we observe features (peaks or inflection points) at low temperatures for the hexapeptides with phase separation promoting residues. The low-temperature peaks arise from competing structural motifs for a relatively small number of low-lying local minima. Peaks can be assigned to competition between these minima using the temperature derivative of the occupation probability (Wales, 2017). The theory provides an exact decomposition of C_V in terms of local minima within the same approximation, which reveals the important cases of interest, where the peaks arise from competition between a few low-energy conformations. We emphasise that peaks in C_V are simply being used as a diagnostic of the structure in the underlying landscape. This structure is clear in the harmonic normal mode approximation to the partition function; a more accurate treatment of C_V is not required to achieve this diagnostic.

The degree of frustration (Bryngelson and Wolynes, 1987; Onuchic and Wolynes, 2004) of the potential energy landscape, quantified via a frustration metric (De Souza *et al.*, 2017), reveals the persistence of high energy barriers separating low-lying minima. In other words, the frustration reflects the existence of competing configurations. The frustration is caused by different low-lying potential energy minima separated by significant barriers. Here, we find that the landscape is more frustrated for the peptides that contain residues (Y/R) with a higher propensity for phase separation, compared to the residues with a lower phase separation propensity. This observation agrees with the finding that the potential energy landscapes for intrinsically disordered proteins are multi-funnelled (Chebaro *et al.*, 2015). However, the frustration metric (De Souza *et al.*, 2017) alone is not sufficient to predict phase separation propensity. Overall, we observe that the peptides with residues that have high phase separation propensity have distinct peaks or inflection points at low temperatures (significantly below the melting temperature) in C_V plots and more frustrated potential energy landscapes. These features in C_V correspond to competing structures stabilised by alternative interactions (aromatic–aromatic or cation–aromatic), or where the residues are oriented differently. This analysis suggests that the calorimetric criterion is a necessary but not a sufficient condition for phase separation (Zhou *et al.*, 1999). The frustration metric provides an additional diagnostic to compare the phase separation propensity of residues in sequences that already exhibit features in C_V at low temperatures.

Methods

The workflow adopted during the current study is presented in Fig. 1 and summarised below. The peptide sequences are constructed using the stickers-and-spacers model (Holehouse and Pappu, 2018b), and the hexapeptides are modelled using the FF99IDPs (Case *et al.*, 2005; Wang *et al.*, 2014) force field (Step 1, Fig. 1). The FF19SB (Tian *et al.*, 2020) potential was also tested for some of the peptides to ensure that the structures represented by C_V features depend on the interactions within the sequence and not on the force field (Supplementary Material). The potential energy landscape is then explored using basin-hopping parallel tempering (BHPT; Step 2, Fig. 1) (Li and Scheraga, 1987, 1988; Wales and Doye, 1997; Strodel *et al.*, 2010). Discrete path sampling (Wales, 2002) is employed to find the connected pathways between local minima (Step 3, Fig. 1). The convergence of sampling is monitored via disconnectivity graphs (Becker and Karplus, 1997; Wales *et al.*, 1998) and heat capacities. The C_V analysis is performed using the harmonic superposition approximation (Step 4, Fig. 1) (Wales, 2017), and the frustration in the landscape is quantified via a frustration metric (De Souza *et al.*, 2017).

Peptide model using AMBER

The hexapeptides are modelled using a properly symmetrised (Malolepsza *et al.*, 2010) version of the FF99IDPs (Wang *et al.*, 2014) force field along with an implicit solvent model (igb = 8), and a monovalent ion concentration of 0.1 M (Case *et al.*, 2005, 2022). The N- and C-terminals are methylated and

https://doi.org/10.1017/qrd.2023.5 Published online by Cambridge University Press

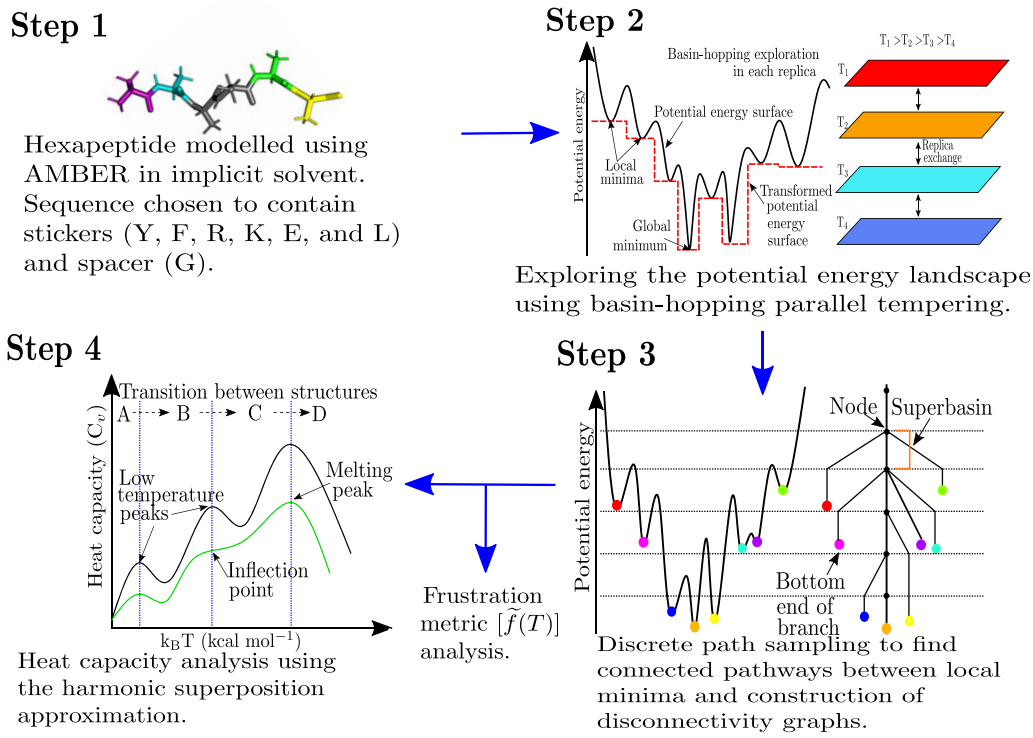

Figure 1. Schematic figure representing the workflow for the computational potential energy landscape exploration to interrogate peptides of varying phase separation propensities.

methylamidated, respectively, to cap the charges in the zwitterionic form of the peptide (Step 1, Fig. 1). We also tested another force field, FF19SB (Tian *et al.*, 2020), and the uncapped peptides for both the force fields. The corresponding results are presented in the Supplementary Material.

Basin-hopping parallel tempering

The global optimisation program GMIN (Wales, 2023a) is used to perform basin-hopping (Wales and Doye, 1997; Strodel *et al.*, 2010; Li and Scheraga, 1987, 1988). For the current computation, the AMBER interface with GMIN is employed. A total of 16 replicas are used with temperatures exponentially distributed between 300 and 575 K. The exchanges are attempted at random with a mean frequency of 10, that is, an average of one exchange every 10 steps. The potential energy landscape is explored by performing 100,000 Cartesian coordinate steps and group rotation (Mochizuki *et al.*, 2014) moves for the side chains. The local minima with C_α in D-form and peptide bonds as *cis*-isomer are discarded. A root-mean-square (RMS) force convergence criterion of 10^{-7} kcal/(mol Angstrom) is employed to save the 400 lowest energy structures differing by at least 0.01 kcal mol^{-1} (to ensure uniqueness of local minima) after running BHPT (Step 2, Fig. 1) (Strodel *et al.*, 2010).

Discrete path sampling

Discrete path sampling (Wales, 2002) implemented in the OPTIM (Wales, 2023b) and PATHSAMPLE (Wales, 2023c) programs is used to find optimal pathways between the local minima and the global minimum. A discrete path is defined as an elementary rearrangement between a local minimum, transition state, and another local minimum. The local minimum is defined as a stationary point with no negative Hessian eigenvalues, whereas a transition state is a first-order saddle point with exactly one negative Hessian eigenvalue (Murrell and Laidler, 1968; Wales, 2003). The doubly-nudged (Trygubenko and Wales, 2004) elastic-band algorithm (Henkelman and Jónsson, 2000; Henkelman *et al.*, 2000) is used to generate candidate transition states, which are then refined accurately using hybrid eigenvector-following (Munro and Wales, 1999). Approximate steepest-descent is employed to find the local minima connected by the transition state using the limited-memory Broyden–Fletcher–Goldfarb–Shanno (L-BFGS) algorithm (Nocedal, 1980; Liu and Nocedal, 1989). Dijkstra's shortest path algorithm (Dijkstra, 1959) is then used to choose the next pair of minima for which a new connection attempt is made, and the process is repeated until a fully connected pathway is found between the minima of interest using the missing connection algorithm (Carr *et al.*, 2005). In the case of some peptides, chain crossing is observed. For these peptides, quasi-continuous interpolation (QCI) (Wales and Carr, 2012; Röder and Wales, 2018) is employed to find the correct pathways. Finally, the stationary point database is optimised using the UNTRAP procedure (Strodel *et al.*, 2007) in PATHSAMPLE to remove artificial frustration in the landscape; that is, low-lying minima separated by large barriers where a lower energy transition state exists. The convergence of the stationary point database is monitored by the convergence of low-temperature peaks in C_V plots, and by analysing the disconnectivity graph (Step 3, Fig. 1).

Disconnectivity graphs

The potential energy landscape of a system of N atoms lies in a $(3N+1)$-dimensional space. Disconnectivity graphs provide a powerful way to visualise the multi-dimensional potential energy landscape (Becker and Karplus, 1997; Wales *et al.*, 1998). They

https://doi.org/10.1017/qrd.2023.5 Published online by Cambridge University Press

preserve the information about the minimum barrier for transitions between minima. The vertical axis of the disconnectivity graph represents the potential (or free) energy. The nodes on the vertical axis represent superbasins composed of disjoint sets of minima. Minima lying within the same superbasin can interconvert via a barrier less than or equal to the energy represented by the superbasin. Each branch originates from a node representing the superbasin and terminates at the energy of a local minimum corresponding to a single branch (Step 3, Fig. 1).

Heat capacity analysis

The harmonic superposition approximation (which is accurate at low temperatures) can be used to express the total partition function as a sum of partition functions of all the local minima. The individual partition functions for the local minima are obtained using normal mode analysis, which yields the harmonic approximation to the vibrational density of states. C_V can now be expressed in terms of occupation probabilities of local minima and their temperature derivatives (Wales, 2017), that is,

$$\begin{aligned} C_V &= \kappa k_B + k_B T^2 \sum_\alpha g_\alpha(T) \left(\frac{\partial \ln p_\alpha(T)}{\partial T} \right) \\ &= \kappa k_B + \sum_\alpha^{g_\alpha(T)<0} g_\alpha(T)(V_\alpha - \langle V \rangle_{min}) + \sum_\alpha^{g_\alpha(T)>0} g_\alpha(T)(V_\alpha - \langle V \rangle_{min}) \\ &\equiv \kappa k_B + C^-(T) + C^+(T). \end{aligned}$$

Here, C_V is the heat capacity, $\kappa = 3N - 6$ is the number of vibrational degrees of freedom for a system of N atoms, k_B is the Boltzmann constant, $g_\alpha(T) \equiv \partial p_\alpha(T)/\partial T$ is the derivative of the occupation probability p_α for minimum α with respect to temperature T, V_α is the potential energy of minimum α, and $\langle V \rangle_{min}$ is the mean potential energy of the minima. The peaks in C_V represent transitions between states with decreasing ($g_\alpha(T) < 0$) and increasing ($g_\alpha(T) > 0$) occupation probability (Wales, 2017).

Frustration metric calculation

Competing low-energy minima separated by significant barriers make the potential energy landscape frustrated. The frustration of the potential energy landscape can be quantified using a frustration metric ($\tilde{f}(T)$), which is a function of temperature:

$$\tilde{f}(T) = \sum_{\alpha \neq gmin} \frac{p_\alpha^{eq}(T)}{1 - p_{gmin}^{eq}(T)} \left(\frac{V_\alpha^\dagger - V_{gmin}}{V_\alpha - V_{gmin}} \right).$$

Here, $\tilde{f}(T)$ is the frustration metric at temperature T, V_{gmin} is the potential energy of the global minimum in the database, V_α is the potential energy of minimum α, $V_\alpha^\dagger$ is the potential energy of the highest energy transition state on the lowest energy pathway between α and the global minimum, and p_α^{eq} and p_{gmin}^{eq} are the equilibrium occupation probabilities of minimum α and the global minimum, which are calculated using the harmonic vibrational density of states. The global minimum does not contribute to frustration and its inclusion leads to an erroneous decrease in frustration at low temperature. Hence, the global minimum is excluded from the frustration metric calculation and occupation probabilities of the remaining minima are renormalised (De Souza *et al.*, 2017).

Results and discussion

The importance of multivalency (Li *et al.*, 2012), interaction strength (Asherie *et al.*, 1996; Das and Pappu, 2013; Hyman *et al.*, 2014; Brangwynne *et al.*, 2015; Choi *et al.*, 2020), and accessibility (Ruff *et al.*, 2022) of stickers in promoting phase separation is well established. Here, we explore the energy landscapes (Fig. 2) of various hexapeptides containing a pair of

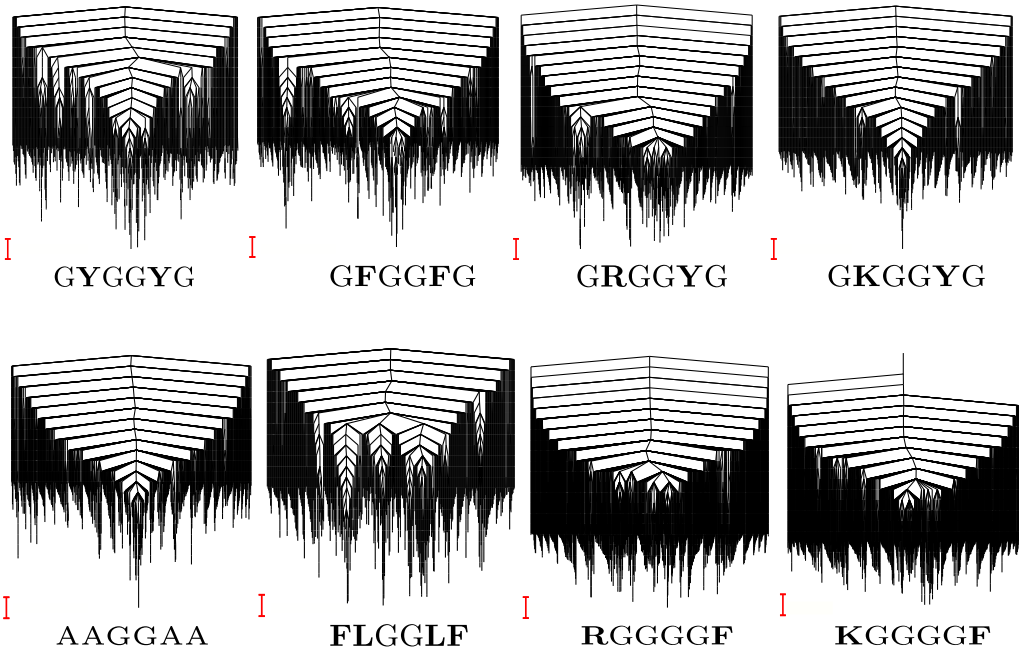

Figure 2. Representative disconnectivity graphs (Becker and Karplus, 1997; Wales *et al.*, 1998) for some of the peptides studied. The scale bar is 1 kcal mol^{-1}.

https://doi.org/10.1017/qrd.2023.5 Published online by Cambridge University Press

dipeptide stickers separated by a GG spacer. The dipeptide stickers include FF, YY, RY, KY, YR, YK, RE, KE, FL, LF, and LL (Abbas *et al.*, 2021). These sequences are chosen to encode the aromatic–aromatic, cation–aromatic, cation–anion and CH–π interactions. The interactions between individual pairs of amino acids are further interrogated by analysing hexapeptides with a pair of stickers separated by two or four glycines. Energy landscapes are also explored for poly-amino acid hexapeptides containing a single type of amino acid residue, including alanine (A), glycine (G), valine (V), arginine (R) and lysine (K). The peptides containing residues with better phase separation propensity show clear features in C_V at low temperatures (Fig. 3*a*, see section "Heat capacity at low temperature"). These features are caused by competing low-energy conformations with different types of interactions (Figs 4 and 5, see section "Interactions leading to features in C_V"). Further analysis of frustration reveals that the peptides with amino acids encoding better phase separation propensity result in more frustrated landscapes (Fig. 3*b*, see section "Frustration in the energy landscape"). It is hypothesised that the collective behaviour of phase separation may be understood in terms of single-molecule properties by quantifying the heat capacity and frustration within the energy landscape

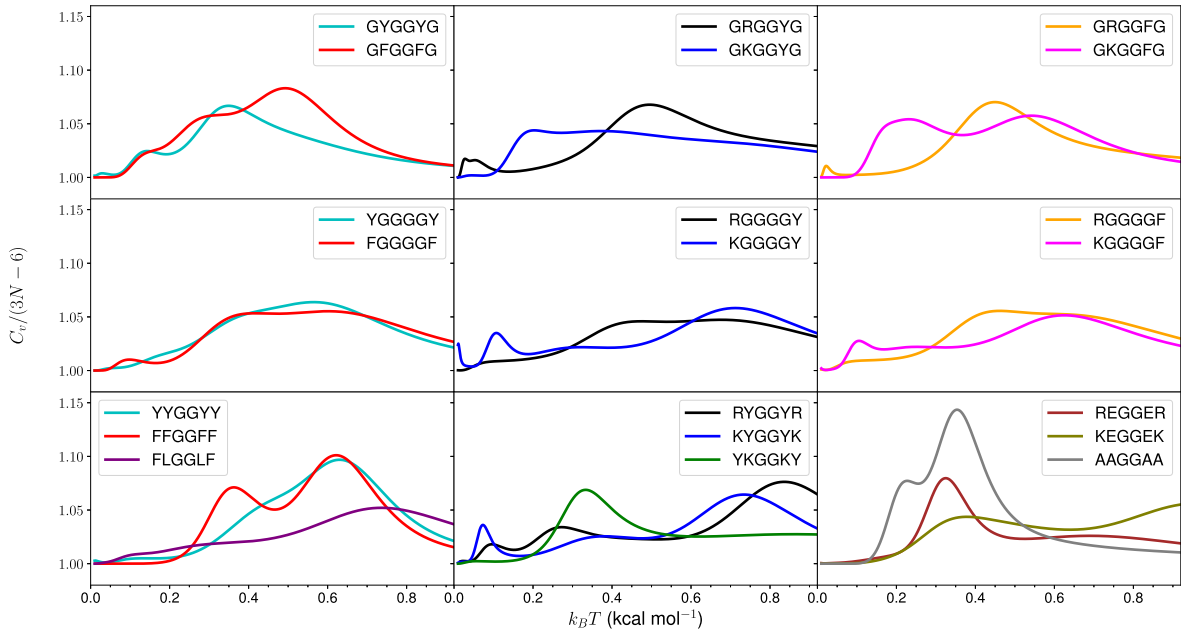

(a) Heat capacity in kcal/(mol K) versus k_BT in kcal mol^{-1} for various hexapeptides.

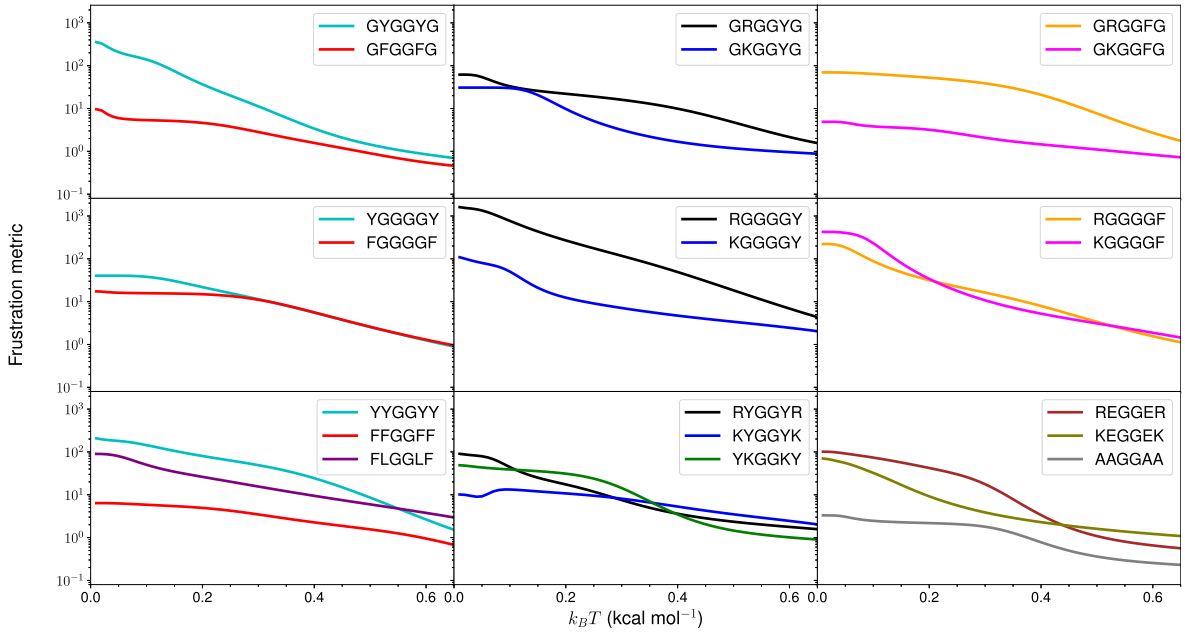

(b) Frustration metric $[\widetilde{f}(T)]$ (De Souza et al., 2017) versus k_BT in kcal mol^{-1} for various hexapeptides.

Figure 3. Heat capacity and frustration metric diagnostic for probing phase separation propensity encoded by different amino acid residues.

https://doi.org/10.1017/qrd.2023.5 Published online by Cambridge University Press

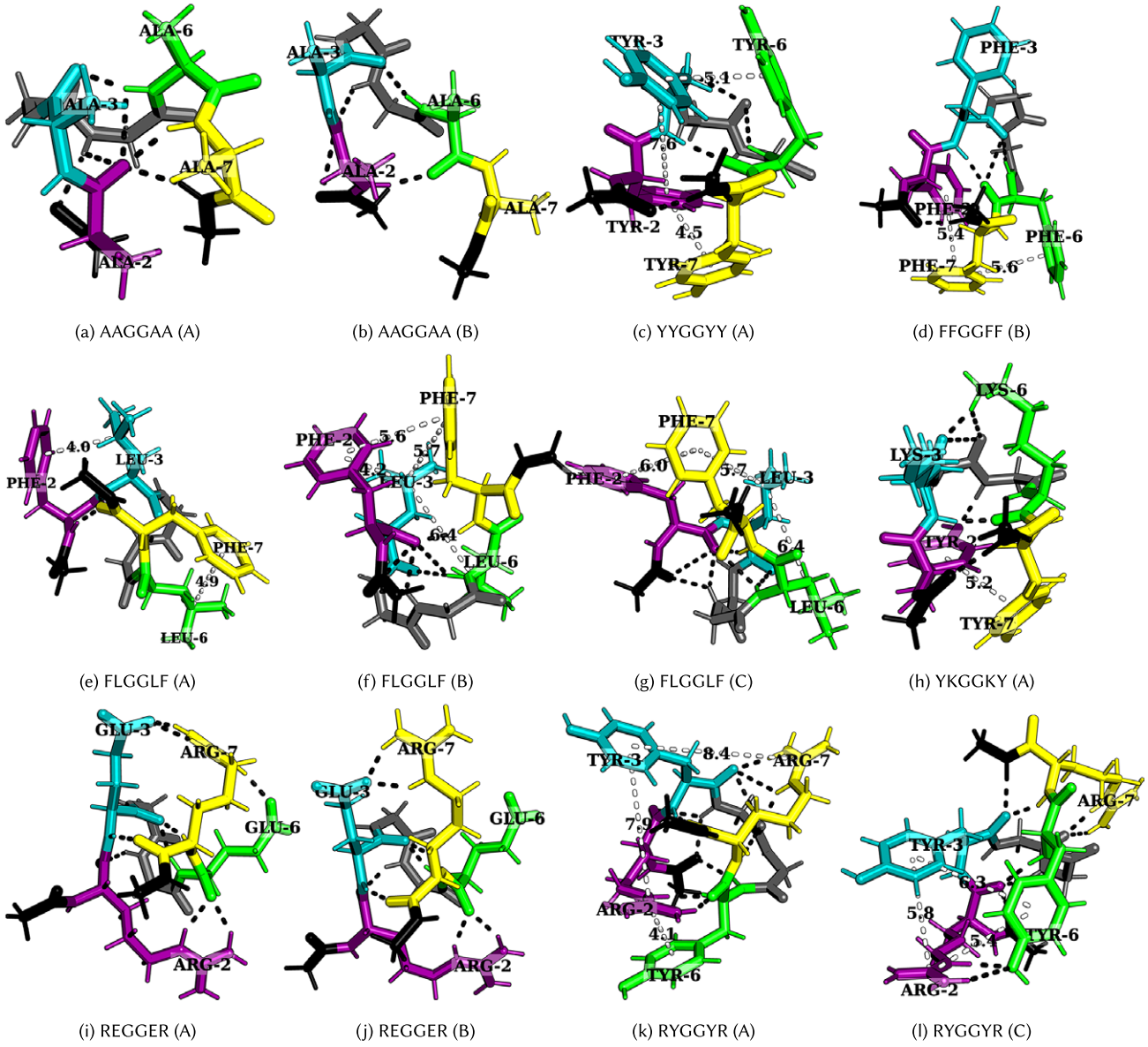

Figure 4. Structures corresponding to low-temperature heat capacity features. The first and second peaks correspond to the transition from A to B and then from B to C, respectively.

framework. An interesting analogue is how the existence of different conformations leads to polymorphic forms for various organic and inorganic molecules (Supplementary Material). A recent study has also shown links between heat capacity change during unfolding and multicomponent phase separation behaviour (Rana *et al.*, 2023).

Heat capacity at low temperature

We first investigate the geometric and energetic parameters that underlie the structural differences represented by low-temperature peaks in the heat capacity of peptides with varying phase separation propensities (Fig. 3*a*). We emphasise that we are using these features as a diagnostic for competing structures in the energy landscape, which may correlate with phase separation propensity. This computational construction does not need to be an accurate calculation of C_V, nor does it need to be experimentally accessible. These peaks represent the transition between competing structures that have significant enthalpic and entropic differences and the integral over the peak represents the latent heat for this transition. In some C_V plots, instead of distinct peaks, we observe inflection points (GFGGFG, YGGGGY, RGGGGY, RGGGGF, YYGGYY, and FLGGLF) where the curvature of the plot changes. These inflection points (or shoulders) may be caused by overlapping peaks. The temperatures corresponding to these distinct inflection points are also considered, since they may contain useful information. The hexapeptide AAGGAA is taken as the control, as it is predicted to have the lowest phase separation propensity of the set (Wang *et al.*, 2018), and the corresponding C_V is simpler (the potential energy landscape is not frustrated) compared to other peptides with more phase separation promoting residues. Note that it is not the height of the peaks but the

https://doi.org/10.1017/qrd.2023.5 Published online by Cambridge University Press

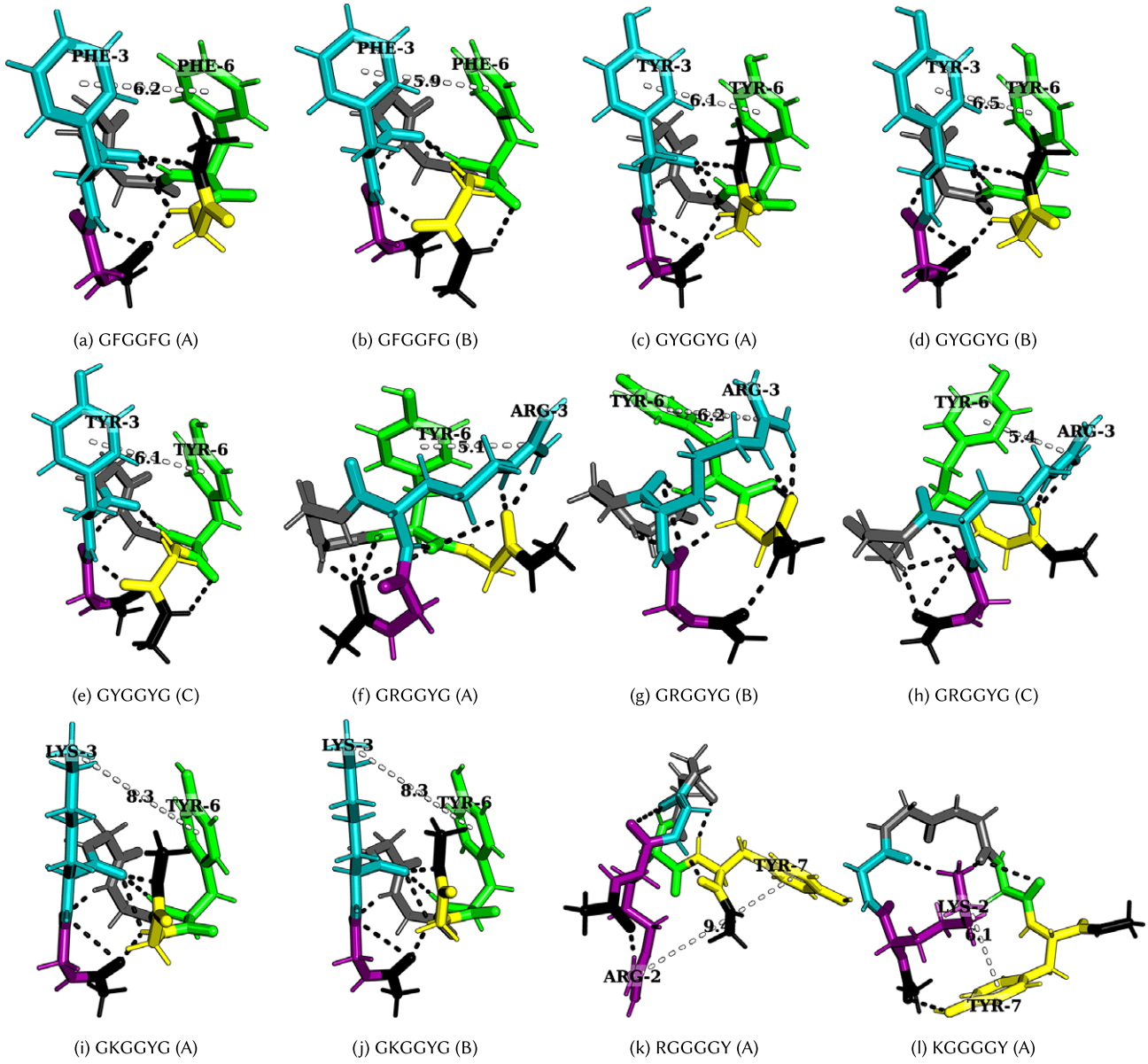

Figure 5. Structures corresponding to low-temperature heat capacity features. The first and second peaks correspond to the transition from A to B and then from B to C, respectively.

existence of features at low temperature (below the melting temperature) that report on the structural heterogeneities in the landscapes, and hence, the phase separation propensities of the constituent residues in a sequence.

Various other hexapeptides, such as GGGGGG, AAAAAA, VVVVVV, EEEEEE, RRRRRR, and KKKKKK, have also been analysed as controls and are found to show simpler C_V profiles (Supplementary Material). However, distinct polar contacts between the main-chain atoms or between the main-chain and side-chain atoms can produce features in C_V (AAGGAA in Fig. 4*a*,*b*).

In general, for hexapeptides with interactions that encode a higher propensity for phase separation, we observe more pronounced features (several distinct peaks and inflection points) in C_V. The frustration metric can then be used as a further diagnostic. The C_V plots for various other peptides are given in the Supplementary Material.

Interactions leading to features in C_V

A low-temperature heat capacity peak often arises from a transition from a compact structure with two sets of dominant interactions between four residues (YYGGYY – Fig. 4*c* and FLGGLF – Fig. 4*e*) to another structure with a similar set of interactions, but with residues oriented differently, or a relatively extended structure with two sets of dominant interactions between three residues (FFGGFF – Fig. 4*d* and FLGGLF – Fig. 4*f*,*g*). Depending on the number of stickers in the peptide, the low-temperature peak may also correspond to a transition from two sets of dominant interactions between three residues to a single principal interaction between two residues (KEGGEK and REGGER – Fig. 4*i*,*j*). A detailed discussion of the competing structures for various hexapeptides is given below.

Tyrosine versus phenylalanine: The presence of a hydroxyl group in tyrosine not only enhances its hydrogen-bonding ability, but also

https://doi.org/10.1017/qrd.2023.5 Published online by Cambridge University Press

results in different rotamers, leading to features in C_V at low temperatures (GYGGYG and YGGGGY). GFGGFG and GYGGYG exhibit inflection points and distinct peaks at low temperatures, respectively. In particular, the low-temperature feature in GFGGFG and FGGGGF corresponds to the transition between a structure with methyl–aromatic and aromatic–aromatic interactions to a structure with an aromatic–aromatic interaction, which further changes to a structure with several polar contacts between distinct atoms. In contrast, for GYGGYG and YGGGGY, the features at low temperature correspond to the transition between rotamers of the aromatic ring containing methyl–aromatic and aromatic–aromatic interactions. Here, the methyl group belongs to the C-terminal cap of the peptide. Interestingly, the observation of a low-temperature peak resulting from the presence of ring rotamers can be compared to an experimental observation in which a bulge in the C_V plot of polystyrene was attributed to the rotation of the phenyl ring around the chain axis (Warfield and Petree, 1962). The orientation that optimises the aromatic interaction depends on the distance between the C_α atoms, stacked at a short distance and T-shaped at a longer distance (Hunter *et al.*, 1991; Chelli *et al.*, 2002). Offset-stacked structures can also be energetically favourable (Ninković *et al.*, 2014), and the methyl group of the cap can also interact with an aromatic residue (Zanuy *et al.*, 2004). We observe similar edge-to-face, CH–π, and methyl–aromatic interactions for GFGGFG (Fig. 5*a*,*b*), GYGGYG (Fig. 5*c*–*e*), FGGGGF, and YGGGGY.

Arginine versus lysine: GRGGYG exhibits features in C_V because of the interaction between R and Y, and the presence of ring rotamers (rotamer of an aromatic ring) for Y (Fig. 5*f*–*h*), whereas for GKGGYG and GKGGFG, it is the methyl group in the C-terminal cap that preferably interacts with the Y/F (Fig. 5*i*,*j*). We still see features in C_V for GKGGYG because of ring rotamers for Y. In the case of RYGGYR, one of the peaks corresponds to the structural transition between the aromatic–cation–aromatic interaction motif to the aromatic–cation interaction motif (Fig. 4*k*,*l*). Hence, R has more propensity than K to interact with the aromatic residues.

Context-dependence: Phase separation may be regarded as a percolation network transition (Mittag and Pappu, 2022). In other words, the formation of a stable condensate occurs when biomolecules interconnect with one another forming a percolated network; the denser the connectivity of the percolated network, the higher the stability of the condensates (Espinosa *et al.*, 2020). The difference in size, the steric packing of R and K, the number of spacers between the stickers, and the distance between the stickers may be useful in explaining the context-dependent properties of these amino acid residues in terms of accessibility and networking ability of stickers to interact with each other. Consider the peptides RYGGYR, GRGGYG, GKGGYG, RGGGGY, and KGGGGY. Even though the presence of R leads to more features in the C_V plots, we observe that when the cationic and aromatic residues are far apart, as for RGGGGY and KGGGGY, K seems to be more flexible and less sterically inhibited, and therefore, it can interact well with Y, whereas R seems to be more rigid and does not interact favourably with Y/F (Fig. 5*k*,*l*). Previous reports suggest that K/RNA coacervates are more dynamic than R/RNA coacervates (Ukmar-Godec *et al.*, 2019), and the R-rich motif may act as a phase disruptor (Odeh and Shorter, 2020). While the different behaviours of R and K may be understood in terms of the relative strength of the interactions, it is also possible that the flexible nature of K compared to R may play a role. Furthermore, the shuffling of sequence may alter the presence of charged residues near the N-/C-termini, which may lead to differences in the properties of these peptides because of the charge interaction with the peptide dipole. The dipole moment effect is expected to be more significant in the case of an uncapped peptide in zwitterionic form (Marqusee and Baldwin, 1987; Tkatchenko *et al.*, 2011).

Aromatic–aromatic versus cation–aromatic interactions: Favourable cation–aromatic interactions between R and Y are observed in RYGGYR (Fig. 4*k*,*l*). However for YKGGKY, the aromatic–aromatic interaction between two tyrosine residues is preferred over the cation–aromatic interaction between K and Y (Fig. 4*h*). This observation hints at the role played by the proximity of interacting residues in a sequence, that is, the two tyrosine residues located at the ends can establish an aromatic–aromatic interaction, which is preferred over the weaker interaction offered by the lysine residues. From a broader perspective, this result may be useful in understanding the context-dependent properties of amino acid residues across different sequences.

Cation–anion interaction: Hydrogen-bonding between oppositely charged amino acids may lead to the formation of salt bridges where the same residue interacts with two different residues (complex) or between two oppositely charged residues (simple) (Musafia *et al.*, 1995). Both REGGER (Fig. 4*i*,*j*) and KEGGEK exhibit low-temperature C_V peaks corresponding to the transition from structures containing a complex salt bridge to a simple salt bridge. The complex salt bridge is formed by the interaction of the same cationic residue with two anionic residues. The next C_V peak at a higher temperature corresponds to the transition from a structure with a cation interacting with a particular anion to a structure with the same cation interacting with a different anion in a different orientation, as in the case of uncapped KEGGEK peptide.

Partial phase separation: Leucine and phenylalanine are constituents of peptides exhibiting partial phase separation (Abbas *et al.*, 2021), and the C_V plot for FLGGLF contains features at low temperatures. The peak represents the transition from a structure containing two distinct pairs of L–F interactions, arising from four residues, to a structure with two pairs of interactions arising from three residues F, F, and L (Fig. 4*e*–*g*). Several CH–π interactions can occur between L and F. Hence, partial phase separation may occur for peptides containing amino acids capable of exhibiting distinct pairs of interactions. However, the interaction strength between stickers is weaker compared to the cation/aromatic–aromatic interaction. Although weak, the CH–π interaction is known to play an important role in supramolecular organisation (Piccolo, 2001).

Frustration in the energy landscape

The frustration (Bryngelson and Wolynes, 1987; Onuchic and Wolynes, 2004) in the multi-dimensional potential energy landscape can be visualised by analysing the multiple funnels in the disconnectivity graph representation (Becker and Karplus, 1997; Wales *et al.*, 1998) (Fig. 2). More funnels with low-energy minima separated by significant barriers from the global minimum make the landscape more frustrated at low temperatures. The frustration is high at very low temperatures because the molecules do not have enough thermal energy to overcome the barrier required for transition from one low-energy conformation to another. In other words, if the state of system corresponds to a low-energy minimum in one funnel, the system is likely to remain in the same funnel when the frustration is high. At higher temperatures the thermal energy is larger and so the molecules have sufficient energy to overcome the barriers and transition between local minima. Hence, the system is less frustrated at higher temperatures. Quantitatively, the frustration metric (De Souza *et al.*, 2017) is generally larger for peptides containing Y/R than for peptides containing F/K at lower temperatures (Fig. 3*b*). In particular, at a very low temperature corresponding to $k_BT = 0.2$ kcal mol^{-1}, the

https://doi.org/10.1017/qrd.2023.5 Published online by Cambridge University Press

frustration metric for GYGGYG is 8 times the value for GFGGFG, YYGGYY is 16 times larger than FFGGFF, GRGGYG is 2 times larger than GKGGYG, GRGGFG is 16 times larger than GKGGFG, and REGGER is 5 times larger than KEGGEK. At $k_BT =$ 0.1 kcal mol^{-1} the frustration metric of RYGGYR is 3 times greater than that of KYGGYK. Hence, it appears that the frustration in the landscape for the monomer peptide directly correlates with the relative phase separation propensity of its constituent residues. This result can also be rationalised by correlating the high frustration with the tendency to be trapped in the unfolded state, and it is well known that unfolded states and intrinsically disordered proteins promote phase separation (Majumdar *et al.*, 2019). Interestingly, KGGGGF is three times more frustrated than RGGGGF at very low temperature ($k_BT =$ 0.1 kcal mol^{-1}). Here, the larger number of spacers (four glycines) increases the distance between the stickers and affects the inaccessibility. The accessibility is reduced more in the case of R, which appears more rigid compared to the more flexible K residue. This difference may explain the context-dependent properties of R in phase-separating proteins. Moreover, the potential energy landscape of FLGGLF is five times more frustrated than FFGGFF at a very low temperature ($k_BT =$ 0.2 kcal mol^{-1}). However, FFGGFF has distinct peaks in the C_V, in contrast to FLGGLF (Fig. 3*a*). These features are caused by a stronger aromatic–aromatic interaction between two F, which correlates with the better phase separation propensity of residues in FFGGFF, whereas the interaction between F and L may facilitate partial phase separation (Abbas *et al.*, 2021). The frustration metric plots for various other peptides are given in the Supplementary Material.

Conclusions

We have investigated the hypothesis that the energy landscape of peptide monomers may report on their phase separation ability, which is a collective phenomenon. The different possible arrangements in which the aromatic–aromatic and cation–aromatic interactions can occur in a peptide monomer can produce low-temperature peaks in the heat capacity. Additionally, the high barriers between the alternative low-lying potential energy minima and the existence of several such conformations, as visualised by multiple funnels in the disconnectivity graph, produce a highly frustrated potential energy landscape. Together, features in the heat capacity plot, and the frustration of the landscape, quantified using the frustration metric, appear to correlate with increased phase separation propensity of the constituent residues. The high frustration results from the molecule being trapped in an intrinsically disordered or unfolded state, and both these states are known to promote phase separation.

This analysis also provides a useful framework to investigate the context-dependent properties of amino acid residues in different sequences. While there have been several attempts (Dzuricky *et al.*, 2020; Simon *et al.*, 2017) to guide the rational design of peptides useful for bioengineering applications, the present study presents a new perspective to design peptides with targeted phase separation behaviour. A related study provides links between the secondary structures that contribute to low-temperature C_V features for monomers and dimers of hexapeptide sequences that are experimentally known to aggregate (Nicy and Wales, 2023). It is important to understand that we are not actually interested in the low-temperature behaviour of the heat capacity and that an accurate calculation is not required. Rather, we are using peaks in an approximate C_V as a computational construction to diagnose competition between alternative favourable structures. It is the characteristics of these conformations that may provide a structural interpretation and diagnostic of higher-order behaviour in condensates, such as liquid–liquid phase separation. Our results suggest that there may indeed be such a connection. We do not claim that this connection is universal, but we do suggest that it may be useful.

Open peer review. To view the open peer review materials for this article, please visit http://doi.org/10.1017/qrd.2023.5.

Supplementary material. The supplementary material for this article can be found at https://doi.org/10.1017/qrd.2023.5.

Data availability statement. The discrete path sampling databases are available at https://doi.org/10.17863/CAM.96972 (Nicy *et al.*, 2023). The step-by-step protocol for creating one such database is given as a tutorial on https://github.com/nicy-nicy/peptide-energy-landscape-exploration. The scripts to analyse the databases can be found at https://github.com/nicy-nicy/energy-landscape-cv-analysis.

Author contribution. J.A.J., R.C.G., D.J.W., and Nicy conceived the idea and designed the study. Nicy performed the simulations and wrote the first draft. All the authors helped with the analysis, interpretation of data and corrected the final draft.

Financial support. This work was supported by Engineering and Physical Sciences Research Council (EPSRC) (D.J.W., Grant No. EP/N035003/1), the Cambridge Commonwealth, European and International Trust, the Allen, Meek and Read Fund, the Santander fund, St Edmund's College, University of Cambridge, and the Trinity-Henry Barlow Honorary Award (Nicy).

Competing interest. The authors declare no competing interest exists.

References

Abbas M, Lipiński WP, Nakashima KK, Huck WTS and Spruijt E (2021) A short peptide synthon for liquid–liquid phase separation. *Nature Chemistry* **13**, 1046–1054.

Asherie N, Lomakin A and Benedek GB (1996) Phase diagram of colloidal solutions. *Physical Review Letters* **77**, 4832.

Banani SF, Lee HO, Hyman AA and Rosen MK (2017) Biomolecular condensates: Organizers of cellular biochemistry. *Nature Reviews Molecular Cell Biology* **18**, 285–298.

Becker OM and Karplus M (1997) The topology of multidimensional potential energy surfaces: Theory and application to peptide structure and kinetics. *Journal of Chemical Physics* **106**, 1495–1517.

Benzinger TH (1971) Thermodynamics, chemical reactions and molecular biology. *Nature* **229**, 100–102.

Boeynaems S, Holehouse AS, Weinhardt V, Kovacs D, Van Lindt J, Larabell C, Van Den Bosch L, Das R, Tompa PS, Pappu RV and Gitler AD (2019) Spontaneous driving forces give rise to protein-RNA condensates with coexisting phases and complex material properties. *Proceedings of the National Academy of Sciences* **116**, 7889–7898.

Bogdan TV, Wales DJ and Calvo F (2006) Equilibrium thermodynamics from basin-sampling. *Journal of Chemical Physics* **124**(4), 044102.

Brady JP, Farber PJ, Sekhar A, Lin Y-H, Huang R, Bah A, Nott TJ, Chan HS, Baldwin AJ, Forman-Kay JD and Kay LE (2017) Structural and hydrodynamic properties of an intrinsically disordered region of a germ cell-specific protein on phase separation. *Proceedings of the National Academy of Sciences* **114**, E8194–E8203.

Brangwynne CP, Eckmann CR, Courson DS, Rybarska A, Hoege C, Gharakhani J, J¨ulicher F and Hyman AA (2009) Germline P granules are liquid droplets that localize by controlled dissolution/−condensation. *Science* **324**, 1729–1732.

Brangwynne CP, Tompa P and Pappu RV (2015) Polymer physics of intracellular phase transitions. *Nature Physics* **11**, 899–904.

Bremer A, Farag M, Borcherds WM, Peran I, Martin EW, Pappu RV and Mittag T (2022) Deciphering how naturally occurring sequence features

impact the phase behaviours of disordered prion-like domains. *Nature Chemistry* **14**, 196–207.

Bryngelson JD and Wolynes PG (1987) Spin glasses and the statistical mechanics of protein folding. *Proceedings of the National Academy of Sciences* **84**, 7524–7528.

Carr JM, Trygubenko SA and Wales DJ (2005) Finding pathways between distant local minima. *Journal of Chemical Physics* **122**, 234903.

Case DA, Cheatham TE, Darden T, Gohlke H, Luo R, Merz KM, Onufriev A, Simmerling C, Wang B and Woods RJ (2005) The Amber biomolecular simulation programs. *Journal of Computational Chemistry* **26**, 1668–1688.

Case DA, Duke RE, Walker RC, Skrynnikov NR, Cheatham III TE, Mikhailovskii O, Simmerling C, Xue Y, Roitberg A, Izmailov SA, *et al.* (2022) AMBER 22 Reference Manual.

Chebaro Y, Ballard AJ, Chakraborty D and Wales DJ (2015) Intrinsically disordered energy landscapes. *Scientific Reports* **5**, 1–12.

Chelli R, Gervasio FL, Procacci P and Schettino V (2002) Stacking and T-shape competition in aromatic–aromatic amino acid interactions. *Journal of the American Chemical Society* **124**, 6133–6143.

Choi J-M, Holehouse AS and Pappu RV (2020) Physical principles underlying the complex biology of intracellular phase transitions. *Annual Review of Biophysics* **49**, 107–133.

Cooper A (2010) Protein heat capacity: An anomaly that maybe never was. *Journal of Physical Chemistry Letters* **1**, 3298–3304.

Das RK and Pappu RV (2013) Conformations of intrinsically disordered proteins are influenced by linear sequence distributions of oppositely charged residues. *Proceedings of the National Academy of Sciences* **110**, 13392–13397.

De Souza VK, Stevenson JD, Niblett SP, Farrell JD and Wales DJ (2017) Defining and quantifying frustration in the energy landscape: Applications to atomic and molecular clusters, biomolecules, jammed and glassy systems. *Journal of Chemical Physics* **146**, 124103.

Dignon GL, Zheng W, Best RB, Kim YC and Mittal J (2018) Relation between single-molecule properties and phase behavior of intrinsically disordered proteins. *Proceedings of the National Academy of Sciences* **115**, 9929–9934.

Dijkstra EW (1959) A note on two problems in connexion with graphs. *Journal of Numerical Mathematics* **1**, 269–271.

Doye JP and Wales DJ (1995) Calculation of thermodynamic properties of small Lennard–Jones clusters incorporating anharmonicity. *Journal of Chemical Physics* **102**, 9659–9672.

Doye JP and Wales DJ (1998) Thermodynamics of global optimization. *Physical Review Letters* **80**, 1357.

Doye JP, Wales DJ and Miller MA (1998) Thermodynamics and the global optimization of Lennard–Jones clusters. *Journal of Chemical Physics* **109**, 8143–8153.

Doye JPK and Calvo F (2002) Entropic effects on the structure of Lennard–Jones clusters. *Journal of Chemical Physics* **116**, 8307–8317.

Dzuricky M, Rogers BA, Shahid A, Cremer PS and Chilkoti A (2020) De novo engineering of intracellular condensates using artificial disordered proteins. *Nature Chemistry* **12**, 814–825.

Espinosa JR, Joseph JA, Sanchez-Burgos I, Garaizar A, Frenkel D and Collepardo-Guevara R (2020) Liquid network connectivity regulates the stability and composition of biomolecular condensates with many components. *Proceedings of the National Academy of Sciences* **117**, 13238–13247.

Finegold L and Cude JL (1972) Specific heat measurements of poly-(l-alanine) at low temperatures (1.8–20 k) and aspects of one dimensionality. *Nature* **237**, 334–335.

Fisher RS and Elbaum-Garfinkle S (2020) Tunable multiphase dynamics of arginine and lysine liquid condensates. *Nature Communications* **11**, 1–10.

Giauque WF and Johnston HL (1929) An isotope of oxygen, mass 17, in the earth's atmosphere. *Journal of the American Chemical Society* **51**(12), 3528–3534.

Greig JA, Nguyen TA, Lee M, Holehouse AS, Posey AE, Pappu RV and Jedd G (2020) Arginine enriched mixed-charge domains provide cohesion for nuclear speckle condensation. *Molecular Cell* **77**, 1237–1250.

Harmon TS, Holehouse AS, Rosen MK and Pappu RV (2017) Intrinsically disordered linkers determine the interplay between phase separation and gelation in multivalent proteins. *Elife* **6**, e30294.

Harmon TS, Holehouse AS and Pappu RV (2018) Differential solvation of intrinsically disordered linkers drives the formation of spatially organized droplets in ternary systems of linear multivalent proteins. *New Journal of Physics* **20**, 045002.

Henkelman G and Jónsson H (2000) Improved tangent estimate in the nudged elastic band method for finding minimum energy paths and saddle points. *Journal of Chemical Physics* **113**, 9978–9985.

Henkelman G, Uberuaga BP and Jónsson H (2000) A climbing image nudged elastic band method for finding saddle points and minimum energy paths. *Journal of Chemical Physics* **113**, 9901–9904.

Holehouse AS and Pappu RV (2018a) Collapse transitions of proteins and the interplay among backbone, sidechain, and solvent interactions. *Annual Review of Biophysics* **47**, 19–39.

Holehouse AS and Pappu RV (2018b) Functional implications of intracellular phase transitions. *Biochemistry* **57**, 2415–2423.

Hunter CA, Singh J and Thornton JM (1991) π-π interactions: The geometry and energetics of phenylalanine-phenylalanine interactions in proteins. *Journal of Molecular Biology* **218**, 837–846.

Hyman AA, Weber CA and Jülicher F (2014) Liquid-liquid phase separation in biology. *Annual Review of Cell and Developmental Biology* **30**, 39–58.

Jonas S and Izaurralde E (2013) The role of disordered protein regions in the assembly of decapping complexes and RNP granules. *Genes & Development* **27**, 2628–2641.

Kabsch W and Sander C (1984) On the use of sequence homologies to predict protein structure: Identical pentapeptides can have completely different conformations. *Proceedings of the National Academy of Sciences* **81**, 1075–1078.

Li P, Banjade S, Cheng H-C, Kim S, Chen B, Guo L, Llaguno M, Hollingsworth JV, King DS, Banani SF, Russo PS, Jiang Q-X, Nixon, BT and Rosen, MK (2012) Phase transitions in the assembly of multivalent signalling proteins. *Nature* **483**, 336–340.

Li Z and Scheraga HA (1987) Monte Carlo-minimization approach to the multiple-minima problem in protein folding. *Proceedings of the National Academy of Sciences* **84**, 6611–6615.

Li Z and Scheraga HA (1988) Structure and free energy of complex thermodynamic systems. *Journal of Molecular Structure: THEOCHEM* **179**, 333–352.

Lin Y, Currie SL and Rosen MK (2017) Intrinsically disordered sequences enable modulation of protein phase separation through distributed tyrosine motifs. *Journal of Biological Chemistry* **292**, 19110–19120.

Liu DC and Nocedal J (1989) On the limited memory BFGS method for large scale optimization. *Mathematical Programming* **45**, 503–528.

Majumdar A, Dogra P, Maity S and Mukhopadhyay S (2019) Liquid–liquid phase separation is driven by large-scale conformational unwinding and fluctuations of intrinsically disordered protein molecules. *Journal of Physical Chemistry Letters* **10**, 3929–3936.

Malinovska L, Kroschwald S and Alberti S (2013) Protein disorder, prion propensities, and self-organizing macromolecular collectives. *Biochimica et Biophysica Acta – Proteins and Proteomics* **1834**, 918–931.

Malolepsza E, Strodel B, Khalili M, Trygubenko S, Fejer S and Wales DJ (2010) Symmetrization of the AMBER and CHARMM force fields. *Journal of Computational Chemistry* **31**, 1402–1409.

Marqusee S and Baldwin RL (1987) Helix stabilization by glu-… lys+ salt bridges in short peptides of de novo design. *Proceedings of the National Academy of Sciences* **84**, 8898–8902.

Martin EW, Holehouse AS, Peran I, Farag M, Incicco JJ, Bremer A, Grace CR, Soranno A, Pappu RV and Mittag T (2020) Valence and patterning of aromatic residues determine the phase behavior of prion-like domains. *Science* **367**, 694–699.

Mittag T and Pappu RV (2022) A conceptual framework for understanding phase separation and addressing open questions and challenges. *Molecular Cell* **82**, 2201–2214.

Mochizuki K, Whittleston CS, Somani S, Kusumaatmaja H and Wales DJ (2014) A conformational factorisation approach for estimating the binding free energies of macromolecules. *Physical Chemistry Chemical Physics* **16**, 2842–2853.

Mrevlishvili GM (1979) Low-temperature calorimetry of biological macromolecules. *Soviet Physics Uspekhi* **22**(6), 433.

Munro LJ and Wales DJ (1999) Defect migration in crystalline silicon. *Physical Review B* **59**, 3969–3980.

https://doi.org/10.1017/qrd.2023.5 Published online by Cambridge University Press

Murrell JN and Laidler KJ (1968) Symmetries of activated complexes. *Transactions of the Faraday Society* **64**, 371–377.

Musafia B, Buchner V and Arad D (1995) Complex salt bridges in proteins: Statistical analysis of structure and function. *Journal of Molecular Biology* **254**, 761–770.

Nicy and Wales DJ (2023) Energy landscapes and heat capacity signatures for monomers and dimers of amyloid-forming hexapeptides. *International Journal of Molecular Sciences* **24**, 10613.

Nicy, Joseph JA, Collepardo-Guevara R and Wales DJ (2023) Research data supporting – Energy landscapes and heat capacity signatures for peptides correlate with phase separation propensity. Apollo – University of Cambridge Repository. https://www.repository.cam.ac.uk/handle/1810/350594

Ninković DB, Andrić JM, Malkov SN and Zarić SD (2014) What are the preferred horizontal displacements of aromatic–aromatic interactions in proteins? Comparison with the calculated benzene–benzene potential energy surface. *Physical Chemistry Chemical Physics* **16**, 11173–11177.

Nocedal J (1980) Updating quasi-newton matrices with limited storage. *Mathematics of Computation* **35**, 773–782.

Nott TJ, Petsalaki E, Farber P, Jervis D, Fussner E, Plochowietz A, Craggs TD, Bazett-Jones DP, Pawson T, Forman-Kay JD and Baldwin AJ (2015) Phase transition of a disordered nuage protein generates environmentally responsive membraneless organelles. *Molecular Cell* **57**, 936–947.

Odeh HM and Shorter J (2020) Arginine-rich dipeptide-repeat proteins as phase disruptors in C9-ALS/FTD. *Emerging Topics in Life Sciences* **4**, 293–305.

Onuchic JN and Wolynes PG (2004) Theory of protein folding. *Current Opinion in Structural Biology* **14**, 70–75.

Pak CW, Kosno M, Holehouse AS, Padrick SB, Mittal A, Ali R, Yunus AA, Liu DR, Pappu RV and Rosen MK (2016) Sequence determinants of intracellular phase separation by complex coacervation of a disordered protein. *Molecular Cell* **63**, 72–85.

Piccolo A (2001) The supramolecular structure of humic substances. *Soil Science* **166**, 810–832.

Poland D (2001) Enthalpy distributions in proteins. *Biopolymers: Original Research on Biomolecules* **58**, 89–105.

Poland D (2002) Contribution of secondary structure to the heat capacity and enthalpy distribution of the unfolded state in proteins. *Biopolymers: Original Research on Biomolecules* **63**, 59–65.

Prabhu NV and Sharp KA (2005) Heat capacity in proteins. *Annual Review of Physical Chemistry* **56**, 521–548.

Qamar S, Wang G, Randle SJ, Ruggeri FS, Varela JA, Lin JQ, Phillips EC, Miyashita A, Williams D, Ströhl F, Meadows, W, Ferry R, Dardov VJ, Tartaglia GG, Farrer LA, Schierle GSK, Kaminski CF, Holt CE, Fraser PE, Schmitt-Ulms G, Klenerman D, Knowles, T, Vendruscolo M and St George-Hyslop P (2018) FUS phase separation is modulated by a molecular chaperone and methylation of arginine cation-π interactions. *Cell* **173**, 720–734.

Quiroz FG and Chilkoti A (2015) Sequence heuristics to encode phase behaviour in intrinsically disordered protein polymers. *Nature Materials* **14**, 1164–1171.

Rana N, Kodirov R, Shakya A and King JT (2023) Protein unfolding thermodynamics predict multicomponent phase behavior. bioRxiv pages 2023–05.

Röder K and Wales DJ (2018) Predicting pathways between distant configurations for biomolecules. *Journal of Chemical Theory and Computation* **14**, 4271–4278.

Ruff KM, Choi YH, Cox D, Ormsby AR, Myung Y, Ascher DB, Radford SE, Pappu RV and Hatters DM (2022) Sequence grammar underlying the unfolding and phase separation of globular proteins. *Molecular Cell* **82**, 3193–3208.

Schmidt HB and Görlich D (2015) Nup98 FG domains from diverse species spontaneously phaseseparate into particles with nuclear pore-like permselectivity. *Elife* **4**, e04251.

Schuster BS, Dignon GL, Tang WS, Kelley FM, Ranganath AK, Jahnke CN, Simpkins AG, Regy RM, Hammer DA, Good MC and Mittal J (2020) Identifying sequence perturbations to an intrinsically disordered protein that determine its phase-separation behavior. *Proceedings of the National Academy of Sciences* **117**, 11421–11431.

Simon JR, Carroll NJ, Rubinstein M, Chilkoti A and López GP (2017) Programming molecular self-assembly of intrinsically disordered proteins containing sequences of low complexity. *Nature Chemistry* **9**, 509–515.

Starkweather HWJ (1960) Heat capacity of chain polymers at low temperatures. *Journal of Polymer Science* **45**(146), 525–527.

Strodel B, Whittleston CS and Wales DJ (2007) Thermodynamics and kinetics of aggregation for the GNNQQNY peptide. *Journal of the American Chemical Society* **129**, 16005–16014.

Strodel B, Lee JW, Whittleston CS and Wales DJ (2010) Transmembrane structures for Alzheimer's Aβ1-42 oligomers. *Journal of the American Chemical Society* **132**, 13300–13312.

Tian C, Kasavajhala K, Belfon KA, Raguette L, Huang H, Migues AN, Bickel J, Wang Y, Pincay J, Wu Q and Simmerling C (2020) ff19sb: Amino-acid-specific protein backbone parameters trained against quantum mechanics energy surfaces in solution. *Journal of Chemical Theory and Computation* **16**, 528–552.

Tkatchenko A, Rossi M, Blum V, Ireta J and Scheffler M (2011) Unraveling the stability of polypeptide helices: Critical role of van der Waals interactions. *Physical Review Letters* **106**, 118102.

Trygubenko SA and Wales DJ (2004) A doubly nudged elastic band method for finding transition states. *Journal of Chemical Physics* **120**, 2082–2094.

Ukmar-Godec T, Hutten S, Grieshop MP, Rezaei-Ghaleh N, Cima-Omori M-S, Biernat J, Mandelkow E, Soding J, Dormann D and Zweckstetter M (2019) Lysine/RNA-interactions drive and regulate biomolecular condensation. *Nature Communications* **10**, 1–15.

Uversky VN, Kuznetsova IM, Turoverov KK and Zaslavsky B (2015) Intrinsically disordered proteins as crucial constituents of cellular aqueous two phase systems and coacervates. *FEBS Letters* **589**, 15–22.

Wales DJ (2002) Discrete path sampling. *Molecular Physics* **100**, 3285–3305.

Wales DJ (2003) *Energy Landscapes: Applications to Clusters, Biomolecules and Glasses*. Cambridge: Cambridge University Press.

Wales DJ (2017) Decoding heat capacity features from the energy landscape. *Physical Review E* **95**, 030105.

Wales DJ (2023a) GMIN: A program for finding global minima and calculating thermodynamic properties from basin-sampling. http://www-wales.ch.cam.ac.uk/GMIN/ (accessed January 26, 2023).

Wales DJ (2023b) OPTIM: A program for optimising geometries and calculating pathways. http://www-wales.ch.cam.ac.uk/software.html (accessed January 26, 2023).

Wales DJ (2023c) PATHSAMPLE: A program for generating connected stationary point databases and extracting global kinetics. http://www-wales.ch.cam.ac.uk/software.html (accessed January 26, 2023).

Wales DJ and Carr JM (2012) Quasi-continuous interpolation scheme for pathways between distant configurations. *Journal of Chemical Theory and Computation* **8**, 5020–5034.

Wales DJ and Doye JPK (1997) Global optimization by basin-hopping and the lowest energy structures of Lennard–Jones clusters containing up to 110 atoms. *Journal of Physical Chemistry A* **101**, 5111–5116.

Wales DJ, Miller MA and Walsh TR (1998) Archetypal energy landscapes. *Nature* **394**, 758–760.

Wang J, Choi J-M, Holehouse AS, Lee HO, Zhang X, Jahnel M, Maharana S, Lemaitre R, Pozniakovsky A, Drechsel D, Poser I, Pappu RV, Alberti S and Hyman AA (2018) A molecular grammar governing the driving forces for phase separation of prion-like RNA binding proteins. *Cell* **174**, 688–699.

Wang W, Ye W, Jiang C, Luo R and Chen H-F (2014) New force field on modeling intrinsically disordered proteins. *Chemical Biology & Drug Design* **84**, 253–269.

Warfield RW and Petree MC (1962) Heat capacity of amorphous polymers at low temperatures. *Nature* **193**, 1280–1281.

Yang Y, Jones HB, Dao TP and Castañeda CA (2019) Single amino acid substitutions in stickers, but not spacers, substantially alter UBQLN2 phase transitions and dense phase material properties. *Journal of Physical Chemistry B* **123**, 3618–3629.

Zanuy D, Haspel N, Tsai H-HG, Ma B, Gunasekaran K, Wolfson HJ and Nussinov R (2004) Side chain interactions determine the amyloid organization: A single layer $_{\beta}$-sheet molecular structure of the calcitonin peptide segment 15–19. *Physical Biology* **1**, 89–99.

Zhou Y, Hall CK and Karplus M (1999) The calorimetric criterion for a two-state process revisited. *Protein Science* **8**, 1064–1074.

https://doi.org/10.1017/qrd.2023.5 Published online by Cambridge University Press